Selected area laser-crystallized polycrystalline silicon thin films by a pulsed Nd:YAG laser with 355 nm wavelength*

Duan Chunyan(段春艳), Liu Chao(刘超), Ai Bin(艾斌), Lai Jianjun(赖键钧), Deng Youjun(邓幼俊), and Shen Hui(沈辉)†

State Key Laboratory of Optoelectronic Materials and Technologies, Institute for Solar Energy Systems, Sun Yat-sen University, Guangzhou 510275, China

Abstract: Selected area laser-crystallized polycrystalline silicon (p-Si) thin films were prepared by the third harmonics (355 nm wavelength) generated by a solid-state pulsed Nd:YAG laser. Surface morphologies of 400 nm thick films after laser irradiation were analyzed. Raman spectra show that film crystallinity is improved with increase of laser energy. The optimum laser energy density is sensitive to the film thickness. The laser energy density for efficiently crystallizing amorphous silicon films is between 440–634 mJ/cm^2 for 300 nm thick films and between 777–993 mJ/cm^2 for 400 nm thick films. The optimized laser energy density is 634, 975 and 1571 mJ/cm^2 for 300, 400 and 500 nm thick films, respectively.

Key words: polycrystalline silicon thin films; Nd:YAG laser; laser crystallization
DOI: 10.1088/1674-4926/32/12/123002 **EEACC:** 2520

1. Introduction

Polycrystalline silicon (p-Si) thin film solar cells are one of the technologies that are most likely to replace traditional bulk silicon solar cells, because they possess advantages of both silicon solar cells (high efficiency, long life, stable performance, using rich and non-toxic raw materials, etc.) and thin film solar cells (less material consumption, low cost). Over the past decade, photovoltaic specialists all over the world have done a lot of research work on this subject[1−11]. The laser annealing technique can be used to induce crystallization of amorphous silicon (a-Si) film to produce p-Si film on low-cost substrates and has become a subject of intense research. Silicon has strong absorption of the shorter wavelengths, such as ultraviolet light and shorter-wavelength visible light. Excimer lasers with ultraviolet wavelengths are widely used[12−15] to crystalize a-Si and fabricate low-temperature p-Si for the thin-film transistors (TFTs). P-Si with several micrometers grains can be obtained using technique of excimer laser recrystallization and masks. However, it has limitations such as high maintenance and operation cost. So solid state lasers, such as Nd:YAG pulsed nanosecond lasers with 532 nm[16−21] and 1064 nm[22−24] have been tried to crystallize a-Si films and prepare microcrystalline silicon. An alternative approach of using a Nd:YAG pulsed laser with 355 nm can be considered because the laser emission wavelength in ultraviolet band is similar to that of excimer lasers and silicon has high absorption coefficient in ultraviolet region. Palani *et al*. used Nd:YAG pulsed nanosecond laser with 355 nm to anneal 400 nm a-Si and got microcrystalline silicon[25].

In this paper, the third harmonics (355 nm wavelength) generated by a solid-state Nd:YAG pulsed picosecond laser without a mask was used to prepare a selected area laser-crystallized p-Si layer with thickness near 300, 400 and 500 nm. Different laser irradiation conditions have been performed to crystallize the a-Si films prepared by magnetron sputtering on glass substrates and the process parameters have been optimized.

2. Experiment

300 nm, 400 nm and 500 nm thick amorphous silicon (a-Si) thin films were deposited on the clean glass substrates by a high-vacuum medium frequency magnetron sputtering system. Silicon with purity of 99.9999% was used as the target and high purity Ar gas as the sputtering gas. The background vacuum of the chamber was about 1×10^{-4} Pa and the substrate temperature during sputtering was 200 ℃.

A 355 nm wavelength laser produced by EKSPLA pulsed Nd:YAG solid-state laser system was used to crystallize a-Si films. The pulse width of the laser is 25 ps and the frequency is 10 Hz. The minimum and maximum energy of a single laser pulse is about 15 μJ and 4.9 mJ, respectively. The laser beam intensity profile was Gaussian with a beam diameter of 6 mm. A diagram of the experimental equipment is shown in Fig. 1. After beam shaping and mirror reflection, the laser passed through a mask with 3 mm diameter round hole and was focalized by one convex with focal length of 50 mm, and projected onto the a-Si thin film sample. The sample was placed on a xy-axis translation stage, with one-dimensional motion (y direction) controlled by a programmable controller which can regulate the movement speed and distance of the stage accurately. The speed can be changed from 0 to 10 mm/s and the movement distance is in the range of 0–100 mm with the minimum step size 0.3 μm and resolution 0.1 μm. The x direction motion

* Project supported by the National Natural Science Foundation of China (Nos. 50802118, 60906005) and the Natural Science Foundation of Guangdong Province, China (No. 9451027501002848).
† Corresponding author. Email: shenhui1956@163.com
Received 7 June 2011, revised manuscript received 11 August 2011

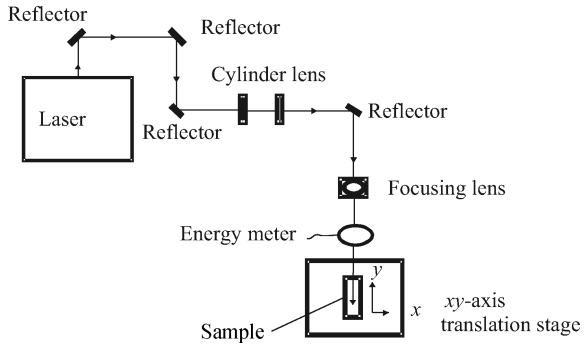

Fig. 1. Diagram of laser-crystallization system.

of the stage is controlled manually, and the movement resolution is 1 μm. By controlling y direction movement speed of the stage on which the sample is fixed, laser scanning speed on the sample can be changed. By adjusting the x direction movement of the stage, the distance between two neighbor columns of laser-crystallized regions on a sample can be adjusted. The experiments were performed at room temperature in air.

A Leica DM2500M microscope and a JSM-6330F scanning electron microscope (SEM) were used to investigate morphology of laser-crystallized a-Si films. A Renishaw laser micro-Raman spectrometer (excitation wavelength 514.5 nm, spectral resolution: 1 cm^{-1}) was used to examine crystallinity of films.

3. Results and discussion

Laser energy density has strong impact on the crystallinity of thin films. When laser energy density is low, a-Si thin films can absorb the laser energy completely. With the increase of laser energy density, much more laser energy is absorbed by the a-Si thin films. When laser energy density reaches a threshold value, the irradiated region starts to melt. With a further increase of laser energy density to an optimum value, the whole irradiated area can be exactly melted, forming high quality recrystallized p-Si thin films.

The a-Si thin film without laser irradiation possesses a smooth surface, but the laser recrystallized region has a rough surface. Films on the edge of the crystallization were partially melted, which form the transition zone between a-Si and p-Si film. Figure 2 gives plane-view SEM images of 400 nm thick a-Si films after laser crystallization and being chemically etched in Sirtl solution ((HF : 5MCrO_3) : 10VH_2O) for 10 s at 25 ℃. No change was observed in the irradiated a-Si film by SEM even using a magnification of 50000 when laser energy density is below 429 mJ/cm^2, which indicates that a-Si film cannot be melted by absorbed laser energy. Some grains appear in the irradiated film surface with laser energy density near 429 mJ/cm^2 (Fig. 2(a)). Grains increased and a-Si islands diminished gradually with the increase of laser energy density. When laser energy density reached 777 mJ/cm^2, the 400 nm a-Si film was melted completely and grains with different sizes were observed in the irradiated film surface (Fig. 2(b)), which shows good crystallinity in the following Raman spectra measurement. Figure 3(b) shows the grain size distribution of 400 nm thick films in Fig. 2(b). It can be seen that 55–75 nm

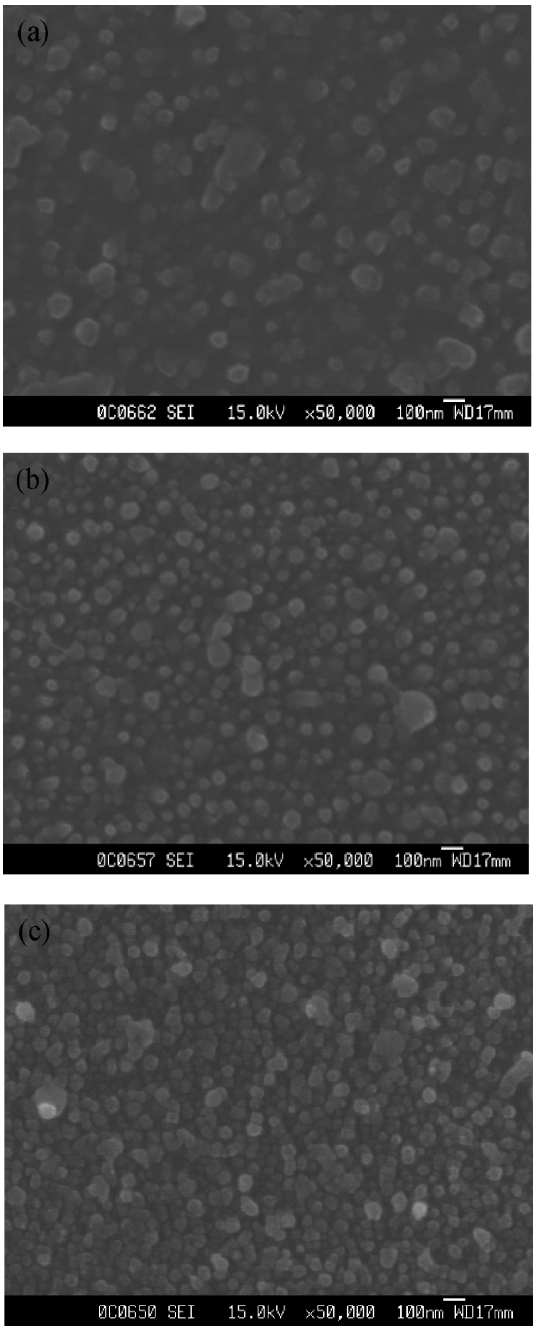

Fig. 2. Surface morphologies of 400 nm thick films after laser crystallization with different laser energy densities. (a) 429 mJ/cm^2. (b) 777 mJ/cm^2. (c) 993 mJ/cm^2.

grains possess 52% of all grains. Agglomeration was observed with laser energy density near 993 mJ/cm^2 (Fig. 2(c)), which might be due to the boiling of molten Si and results in damage to the crystallized film.

3.1. Surface morphology

Figure 3(a) shows the grain size distribution of 300 nm films after laser crystallization with laser energy density near 634 mJ/cm^2. We can see that grains in the region of 65–95 nm in size account for 68%. Grains in 300 nm laser-crystallized films are larger than those in 400 nm laser-crystallized films.

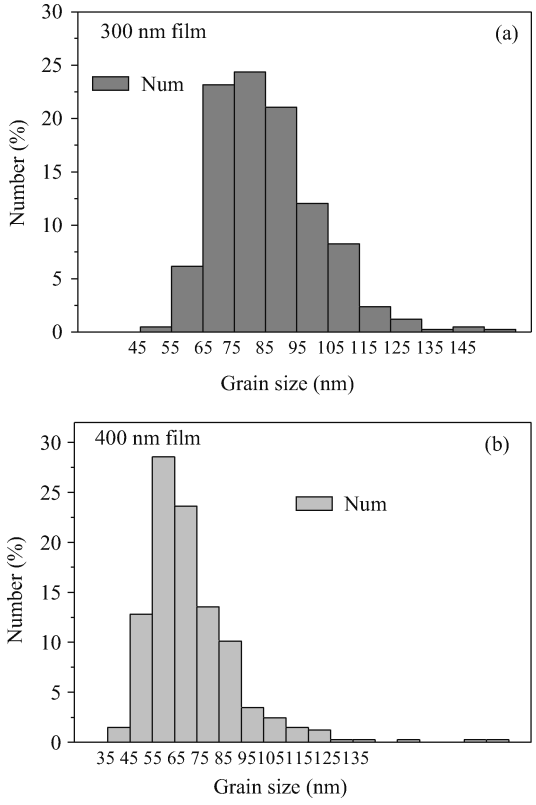

Fig. 3. Grain size distribution of 300 nm and 400 nm thick films after laser crystallization. (a) 300 nm. (b) 400 nm.

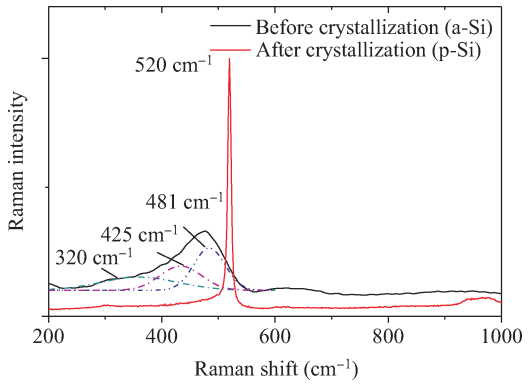

Fig. 4. Raman spectra of the 300 nm a-Si film before and after laser crystallization.

3.2. Analysis of Raman spectra

Raman spectroscopy is quite suitable for distinguishing crystalline silicon (c-Si) phase from a-Si thin films. So the Raman spectra of the films were measured to study the effect of laser energy density on the film crystallinity. Figure 4 shows the Raman spectra of 300 nm a-Si film before and after laser irradiation (634 mJ/cm^2). Before laser crystallization, the Raman spectrum shows three characteristic peaks of a-Si thin films, which are 320, 425, 481 cm^{-1}, respectively. The broad peak near 481 cm^{-1}, which is characteristic of the transverse optic (TO) mode of the a-Si phase[26]. The weak peak near 320 cm^{-1} corresponds to the position of the longitudinal acoustical (LA) phonon of the scattering peak[27]. The

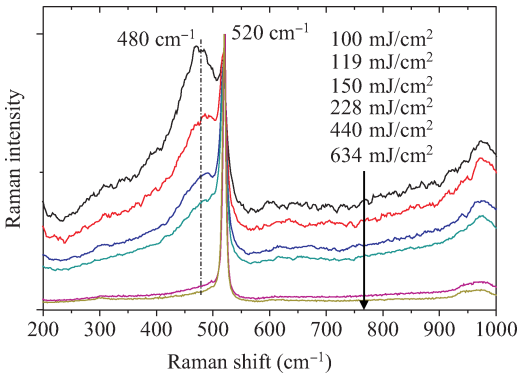

Fig. 5. Raman spectra of the 300 nm a-Si films crystallized by using different energy densities of laser.

peak near 425 cm^{-1} corresponds to the position of the longitudinal optic (LO) phonon peak of the a-Si phase[28]. After laser crystallization, the Raman spectrum demonstrates a narrow and sharp peak near 520 cm^{-1}, which corresponds to the TO mode of c-Si[26–29], indicating that c-Si appears after laser irradiation.

Figure 5 shows Raman spectra of several 300 nm films irradiated by laser with different energy densities. When laser energy density is near 100 mJ/cm^2, the Raman spectrum exhibits a narrow peak at 520 cm^{-1} and a broad peak centred at 480 cm^{-1}, indicating that the film is composed of both a-Si and c-Si. With laser energy density increasing, the intensity of the peak near 480 cm^{-1} decreases, while the intensity of the peak near 520 cm^{-1} increases, which indicates that the film crystallinity improves. When laser energy density reaches 440 mJ/cm^2, the Raman spectrum exhibits a narrow peak at 520 cm^{-1}, which suggests that the film has been completely crystallized. However, the peak shows asymmetry and has a shoulder towards a lower wave number. This shoulder may come from the defective part of the crystalline phase[26]. With further increase of laser energy density, the peak near 520 cm^{-1} becomes much narrower and sharper, which reconfirms that the film crystallinity would improve with increase of laser energy density.

400 nm and 500 nm a-Si films were also crystallized by using different energy densities of laser and scanning speed of 10 mm/s. Figure 6 shows several typical Raman spectra of the 400 nm and 500 nm laser crystallized a-Si films. It can be seen from Fig. 6 that the a-Si films were just partially crystallized when laser energy density is 177 mJ/cm^2 for the 400 nm a-Si films and 236 mJ/cm^2 for the 500 nm a-Si films. With laser energy density increasing, the film crystallinity improves. For instance, an enhancement in the crystallinity of a-Si films of both 500 nm and 400 nm thicknesses were observed by utilizing a laser energy density of 1571 mJ/cm^2 and 975 mJ/cm^2, respectively. However, the peak shows asymmetry and has a shoulder towards lower wave number. It is well known that small grains and regions with high defect densities in p-Si films can result in asymmetry and expansion of the Raman spectrum due to phonon scattering from the microcrystalline boundaries[30–32]. Thus, this shoulder may result from the defective part of the crystalline phase or crystallites. Further increase of laser energy densities to 993 mJ/cm^2 and 2208 mJ/cm^2 for a 400 nm

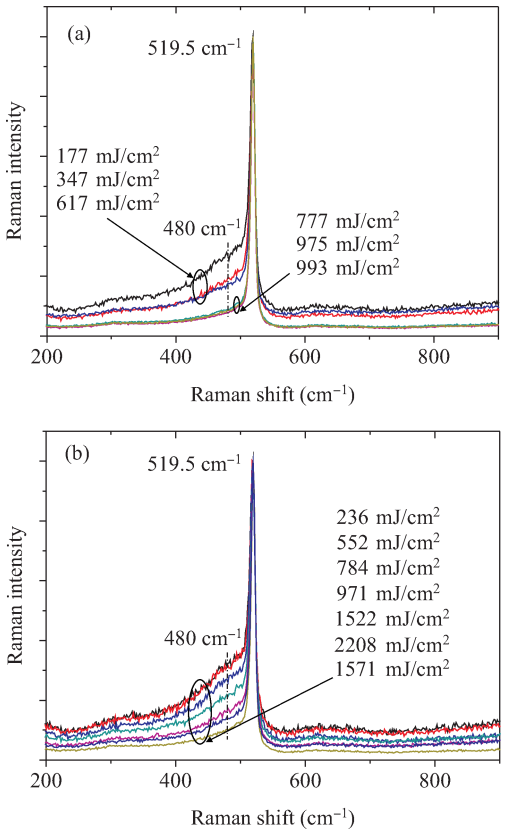

Fig. 6. Raman spectra of (a) the 400 nm and (b) the 500 nm films crystallized by using different energy densities of laser.

and 500 nm a-Si films, respectively, resulted in a degradation of the crystalline quality of the thin films.

It can be concluded from above discussion on the Raman spectra that the larger laser energy density is necessary to crystallize the thicker a-Si films. The optimum laser energy density is also different for the a-Si films with different thicknesses. a-Si films with 300, 400, 500 nm thickness possess better crystallinity when laser energy density is at 634 mJ/cm^2, 975 mJ/cm^2 and 1571 mJ/cm^2, respectively. The crystalline quality of the a-Si film decreases when the laser energy density is above the optimum value. Moreover, the crystalline quality of 300 nm a-Si films crystallized by laser is much better than those obtained on 400 nm and 500 nm a-Si films.

4. Conclusion

The influence of the energy density of a 355 nm laser generated by a solid-state Nd:YAG pulsed picosecond laser on the crystallization of a-Si films sputtered on glass substrates has been experimentally investigated. It was found that different laser energies are needed for crystallizing different thicknesses of a-Si films. The laser energy density for efficiently crystallizing a-Si films is between 440–634 mJ/cm^2 for 300 nm films and between 777–993 mJ/cm^2 for 400 nm films. Raman spectra show that a-Si films with 300, 400, 500 nm thickness possess better crystallinity when the laser energy density is at 634, 975 and 1571 mJ/cm^2, respectively. By adjusting the x and y direction movement of the xy-axis translation stage, the selected area laser-crystallized silicon thin films with different patterns of crystallized regions can be fabricated. In a word, 355 nm laser output by picosecond Nd:YAG laser system is suitable for preparing the selected area crystallized p-Si layers. However, grains in the laser-crystallized films are small for p-Si thin film solar cells and the technique will be further optimized to achieve sequential lateral growth and fabricate p-Si with larger grains with the aid of an optical mask.

Acknowledgements

The authors would like to thank Mr. Zeng Xueran (State Key Laboratory of Optoelectronic Materials and Technologies, Sun Yat-Sen University) for his assistance with the operation of the laser system.

References

[1] Wang J H, Lien S Y, Chen C F, et al. Large-grain polycrystalline silicon solar cell on epitaxial thickening of AIC seed layer by hot wire CVD. IEEE Electron Device Lett, 2010, 31(1): 38

[2] Gall S, Becker C, Conrad E, et al. Polycrystalline silicon thin-film solar cells on glass. Solar Energy Materials and Solar Cells, 2009, 93(6/7): 1004

[3] Focsa A, Gordon I, Auger J M, et al. Thin film polycrystalline silicon solar cells on mullite ceramics. Renewable Energy, 2008, 33(2): 267

[4] Gordon I, Carnel L, Gestel D V, et al. 8% efficient thin-film polycrystalline-silicon solar cells based on aluminum-induced crystallization and thermal CVD. Progress in Photovoltaics, 2007, 15(7): 575

[5] Slaoui A, Pihan E, Focsa A. Thin-film silicon solar cells on mullite substrates. Solar Energy Materials and Solar Cells, 2006, 90(10): 1542

[6] Wang W J, Xu Y, Shen H. Polycrystalline silicon thin-film solar cells on various substrates. Phys Status Solidi A, 2006, 203(4): 721

[7] Zhao Y W, Geng X H, Wang W J, et al. R & D activities of silicon-based thin-film solar cells in China. Phys Status Solidi A, 2006, 203(4): 714

[8] Ai B, Shen H, Liang Z C, et al. Study on epitaxial silicon thin film solar cells on low cost silicon ribbon substrates. J Cryst Growth, 2005, 276(1/2): 83

[9] Yamamoto K, Nakajima A, Yoshimi M, et al. A thin-film silicon solar cell and module. Progress in Photovoltaics, 2005, 13(6): 489

[10] Beaucarne G, Bourdais S, Slaoui A, et al. Thin-film polycrystalline Si solar cells on foreign substrates: film formation at intermediate temperatures (700–1300 ℃). Appl Phys A: Materials Science & Processing, 2004, 79(3): 469

[11] Reber S, Hurrle A, Eyer A, et al. Crystalline silicon thin-film solar cells—recent results at Fraunhofer ISE. Solar Energy, 2004, 77(6): 865

[12] Lengsfeld P, Nickel N H, Genzel C, et al. Stress in undoped and doped laser crystallized poly-Si. J Appl Phys, 2002, 91(11): 9128

[13] Tsunoda I, Matsuura R, Tanaka M, et al. Direct formation of strained Si on insulator by laser annealing. Thin Solid Films, 2006, 508: 96

[14] Zhang F M, Liu X C, Ni G, et al. Controlled growth of high-quality poly-silicon thin films with huge grains on glass substrates using an excimer laser. J Cryst Growth, 2004, 260: 102

[15] Kumomi H. Location control of crystal grains in excimer laser crystallization of silicon thin films. Appl Phys Lett, 2003, 83(3):

434
[16] Jin J, Yuan Z J, Huang L, et al. Laser crystallization of amorphous silicon films investigated by Raman spectroscopy and atomic force microscopy. Appl Surf Sci, 2010, 256: 3453
[17] Yuan Zhijun, Lou Qihong, Zhou Jun, et al. Flat-top green laser crystallization of amorphous silicon thin film. Chinese Journal of Lasers, 2009, 36(1): 205
[18] Ambrosone G, Coscia U, Lettieriv S, et al. Crystallization of hydrogenated amorphous silicon-carbon films by means of laser treatments. Appl Surf Sci, 2005, 247: 471
[19] Liu Jianping, Wang Haiwen, Li Juan, et al. Using a YAG Laser to make poly-silicon. Chinese Journal of Semiconductors, 2005, 26(8): 1572
[20] Tang Y F, Silva S R P, Rose M J. Super sequential lateral growth of Nd:YAG laser crystallized hydrogenated amorphous silicon. Appl Phys Lett, 2001, 78(2): 186
[21] Wohllebe A, Carius R, Houben L, et al. Crystallization of amorphous Si films for thin film solar cells. Journal of Non-Crystalline Solids, 1998, 227–230: 925
[22] Carius R, Wohllebe A, Houben L, et al. Pulsed laser crystallization of a-Si:H on glass: a comparative study of 1064 and 532 nm excitation. Phys Status Solidi A, 1998, 166: 635
[23] Nebel C E, Christiansen S, Strunk H P, et al. Laser-interface crystallization of amorphous Silicon: application and properties. Phys Status Solidi A, 1998, 166: 667
[24] Ferreira I, Carvalho J, Martins R. Undoped and doped crystalline silicon films obtained by Nd-YAG laser. Thin Solid Films, 1998, 317: 140
[25] Palani I A, Vasa N J, Singaperumal M. Crystallization and ablation in annealing of amorphous-Si thin film on glass and crystalline-Si substrates irradiated by third harmonics of Nd^{3+}:YAG laser. Materials Science in Semiconductor Processing, 2008, 11: 107
[26] Droz M C. Thin film microcrystalline silicon layers and solar cells: microstructure and electrical performances. PhD Thesis, Universite de Neuchatel, Switzerland, 2003: 11
[27] Zotov N, Marinov M, Mousseau N, et al. Dependence of the vibrational spectra of amorphous silicon on the defect concentration and ring distribution. J Phys: Condensed Matter, 1999, 11(48): 9647
[28] Ma Zhixun, Liao Xianbo, Kong Guanglin, et al. Raman research of nanosilicon inlaying the oxidized silicon film. Science in China Series A, 2000, 30 (2): 169
[29] Cerqueira M F, Ferreira J A. Temperature dependence of the first order Raman scattering in thin films of μc-Si:H. Journal of Materials Processing Technology, 1999, 92/93: 235
[30] Iqbal Z, Vepiek S, Webb A P, et al. Raman scattering from small particle size polycrystalline silicon. Solid State Commun, 1981, 37(12): 993
[31] Richter H, Wang Z P, Ley L. The one phonon Raman spectrum in microcrystalline silicon. Solid State Commun, 1981, 39(5): 625
[32] Campbell I H, Fauchet P M. The effects of microcrystal size and shape on the one phonon Raman spectra of crystalline semiconductors. Solid State Commun, 1986, 58(10): 739